DESIGN AND CHARACTERIZATION OF THE TENSILE PROPERTIES OF 3-D BRAID-TWIST LIGAMENT SCAFFOLDS

By Rohit Rao

A thesis submitted to the Graduate School – New Brunswick

Rutgers, The State University of New Jersey

and

The Graduate School of Biomedical Sciences

University of Medicine and Dentistry of New Jersey

in partial fulfillment of the requirements for the degree of

Master of Science

Graduate Program in Biomedical Engineering

Written under the direction of

Dr. Joseph Freeman

and approved by

_____

_____

_____

New Brunswick, New Jersey
January 2015

ABSTRACT OF THE THESIS

Design and Characterization of the Tensile Properties of 3-D Braid-Twist Ligament Scaffolds

By: Rohit Rao

Thesis Advisor: Dr. Joseph Freeman

There are roughly between 100,000 -250,000 anterior cruciate ligament (ACL) injuries that are annually diagnosed in the U.S. alone. Around 50,000 of these require surgical reconstruction and replacement of the ACL [1-2]. The current treatment of choice is the use of an autograft harvested from the patellar tendon, the hamstring tendon or quadriceps tendons. However, autologous grafts are associated with a number of drawbacks including donor site morbidity and the requirement of two surgeries to carry out the ACL replacement. Therefore, alternative techniques need to be developed for ACL reconstruction. Recently tissue engineering-based scaffolds have received wide attention as potentially viable alternatives to autografts. This report discusses the development and characterization of the tensile properties of a 3-D braid twist scaffold fabricated using an automated braiding machine. The braiding angle of the scaffolds was altered in a controllable manner. Scaffolds with three different braiding angles; 53°, 63° and 72° were obtained to determine the effect of braiding angle on the tensile properties of the braid-twist scaffolds. Based on these studies scaffolds with a braiding angle of 72° were determined to have tensile characteristics most suitable for ligament replacement. Future studies will further evaluate the mechanical and biological properties of these scaffolds.

ACKNOWLEDGEMENTS

I thank my advisor Dr. Joseph Freeman, for his continual guidance during the course of this project. I also thank my committee members, Dr. Michael Dunn and Dr. Ronke Olabisi for their support and advice. Furthermore, I thank my fellow members of the Musculoskeletal Tissue Regeneration (MoTR) Laboratory, Dr. David Shreiber, the director of the graduate program in Biomedical Engineering and the graduate faculty members of the Biomedical Engineering Department at Rutgers University for their advice and encouragement.

I am grateful to my family and my girlfriend, for their encouragement during the course of my project. Finally, I am thankful to my friends for their support and for helping to make this a very enjoyable experience.

Table of Contents

List of Figures

List of Tables

CHAPTER 1: INTRODUCTION

1.1 Anatomy and Function of the ACL

The ACL is the primary intra-articular ligament of the knee and extends from a broad area on the anterior of the tibia between the intercondylar eminences to a semicircular posteromedial portion of the lateral femoral condyle. The ACL makes a critical contribution to physiological kinematics and stability by preventing excessive anterior tibial translation with respect to the femur while allowing normal helicoid motion of the knee. The ACL has two major fiber bundles called the anteromedial and posterolateral bundle that have characteristic functional features [Figure 1][3-5]. When the knee is extended the posterolateral bundle becomes taut and the anteromedial bundles becomes lax, while the anteromedial bundle becomes taut and the posterlateral bundle relaxes as the knee is flexed [3][6]. Anatomical studies of the ACL reveal that ACL is about 31-38 mm in length and 10-12 mm in width [7], with the average width of anteromedial bundle measuring 6-7 mm and that of the posterolateral bundle measuring 5-6 mm [4][8].

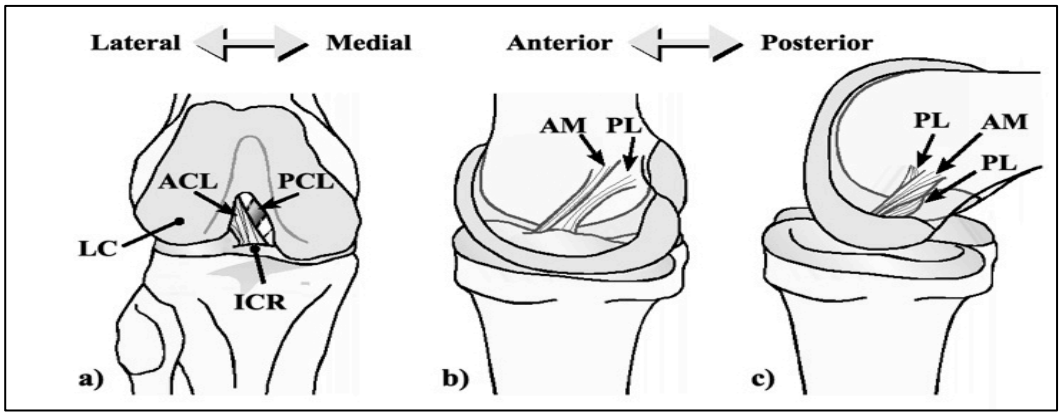

Figure 1: Schematic description of the anatomy of the ACL [5]

The ACL is composed of dense connective tissue is primarily composed of collagen, which accounts for about 75% of the dry weight (85% Type I with varying amounts of types III, V, VI, XI and XIV), proteoglycans (less than 1% of the dry weight), elastin, glycoproteins and other proteins such as actin, laminin and integrins [9]. Furthermore, all ligaments exhibit a hierarchical structure as shown in Figure 2. At the scale of the whole tissue, the ligament is covered by the epiligament, which is often indistinguishable from the bone and merges into the periosteum of the bone near the ligament adjacent to the enthesis [9]. The ligament itself is composed of bundled fascicles that are separated by another layer of connective tissue called the endoligament. The fascicles are in turn made up of collagen fibrils that are oriented along the long axis of the ligament, giving rise to its the anisotropic mechanical properties. Interactions between the collagen fibrils and non-collagenous components and ligament fibroblasts also contribute to the characteristic mechanical properties of the ligament. Furthermore, the collagen fibrils exhibit a periodic crimp patters that repeats every 45-60 μm [10-12]. The fibrils are subsequently composed of collagen microfibrils, which are in turn made of individual collagen molecules arranged in a triple helical configuration.

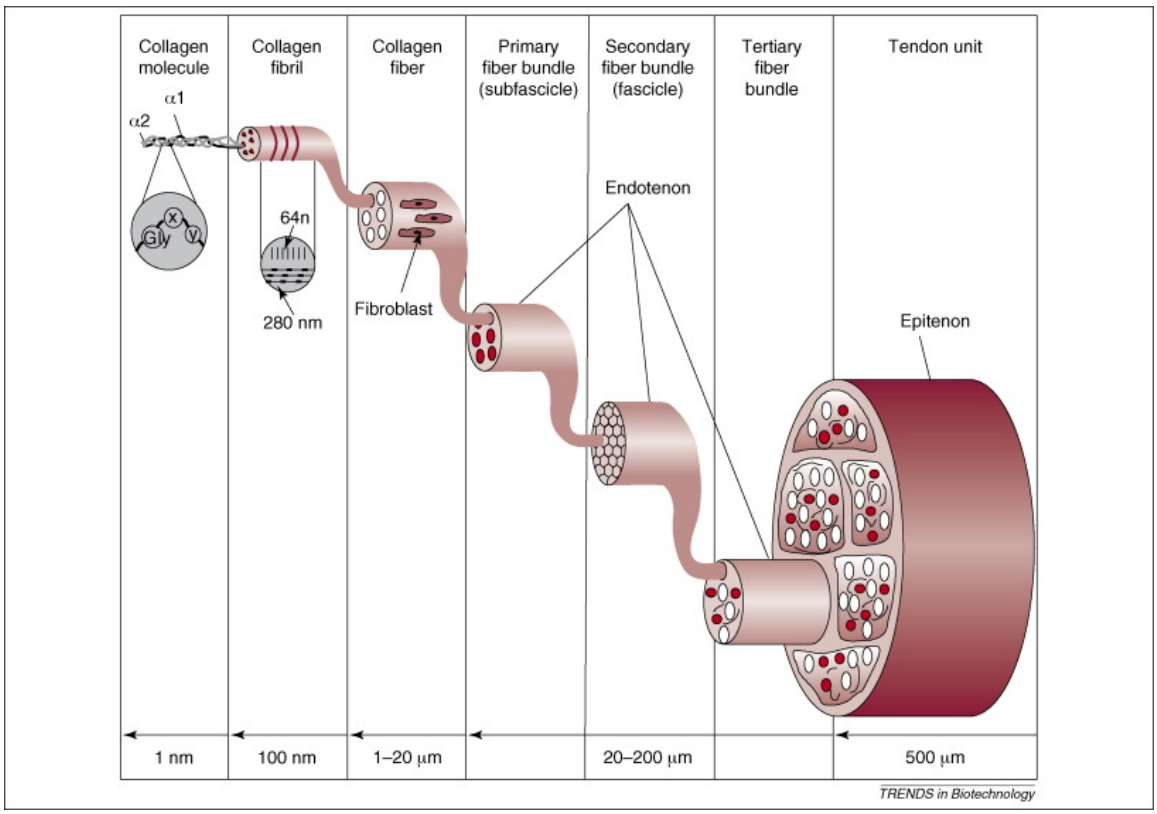

Figure 2: Schematic diagram describing hierarchical structure of tendons and ligaments [13]

1.2 Mechanical Characteristics of Anterior Cruciate Ligament

Ligaments demonstrate viscoelastic strain-rate dependent mechanics and display creep, stress relaxation and hysteresis [14-16]. At constant strain rates, ligaments exhibit a characteristic tri-phasic stress-strain response composed of a toe-region, a linear region and a yield region [Figure 3**]**. The toe-region occurs at low stresses and is characterized by a low stress per unit strain. At a structural level, this region corresponds to the straightening out of crimp pattern of the collagen fibrils. As the stress is increased the collagen fibrils become extended and begin to slide relative to each other. Both the toe region and linear region allow for recoverable deformation with linear region being the stiffer of the two. Finally, the yield region results from a further increase in stress. In this region, the collagen fibrils are fully extended and begin to start rupturing resulting in a

drop in stress with increasing strain, and eventually leading to complete failure of the ligament.

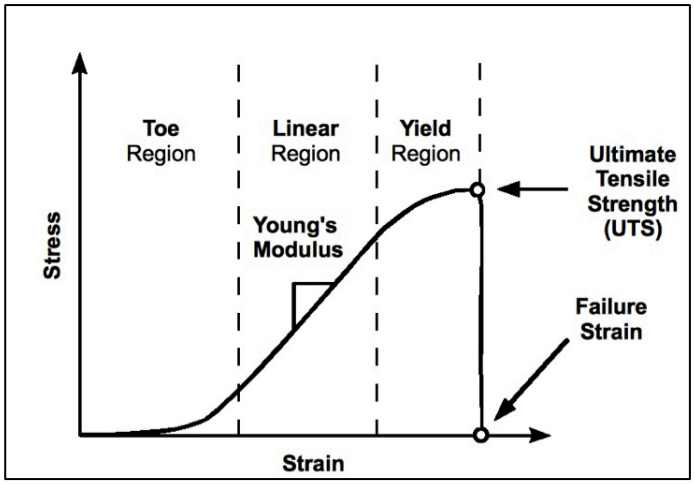

Figure 3: Characteristic stress-strain response of the ACL [17]

1.3 Current Treatments for ACL Injuries

Partial ligament tears can occur when there is excessive translation or rotation of the femur with respect to the tibia. Due to its relatively poor vascularization ligaments have a reduced capacity to heal after injury compared to well-vascularized tissues such as the bone [10]. Partial tears can be treated with rest, short-duration of immobilization, cold compress and by elevation of the leg to drain accumulated fluid from the joint. However, surgical replacement is necessary to treat complete mid-substance tears or when ligament is severed at the site of insertion into the bone. Patients with complete tears run the risk of the suffering from early osteoarthritis if their injury is left untreated [18-19].

Ligament replacements can be broadly categorized into biological grafts and synthetic grafts. Biological grafts include autografts, which are sourced from the patient, and allografts, sourced from donor tissue (or from cadaveric tissue) and xenografts, which are sourced from another species (porcine grafts) [10][20-22].

1.3.1 Biological Grafts

Currently the most common autografts being used for ACL reconstruction are the obtained from sections of the patellar tendon, hamstring tendon and quadriceps tendon [23-24]. The current graft gold standard for ACL reconstruction is the patellar tendon autograft. In this method, the central $1/3^{rd}$ or the lateral $1/3^{rd}$ of the patellar tendon are passed and fixed in tunnels drilled into femur and tibia. The autograft tissue is usually harvested with a part of the bone from the patella and bone from the patellar tendon insertion site that are subsequently used as bone insertions while replacing the ACL. The force at the ultimate tensile strength of this bone-patellar tendon-bone graft is approximately 2950 MPa [25] . The graft is able to withstand future stresses after comprehensive rehabilitation, promote cell proliferation and tissue ingrowth [10][22]. However, the primary drawbacks of this graft are donor site morbidity, requirement of two surgeries; one to harvest the graft tissue and one for the replacement of the ligament, and the associated potential complication of patella fracture. Furthermore, autografts do not perfectly recapitulate the long-term mechanical properties of the native ACL.

1.3.2 Allografts

Similar to autografts, allografts provide initial mechanical support, promote cell proliferation and tissue ingrowth. Additionally, they do not generally suffer from availability problems and eliminate the need for multiple surgeries during the ACL replacement. However, the use of allografts is associated with an increased risk of adverse host immune response following implantation. Further, necessity of sterilization

due to potential for disease transfer generally results in a deterioration of mechanical properties [10] [22].

1.3.3 Xenografts

Xenografts have similar advantages to allografts when compared to autografts. However, xenografts are associated with an even greater susceptibility to disease transmission and hyper-acute immune rejection than allografts. The immune sensitivity of xenografts is generally due to the presence of α-galactose (α-Gal) epitope, and hence, need to be pre-treated to remove α-Gal as well as decellularized prior to implantation [22][26].

1.3.4 Synthetic Grafts

Synthetic implants can be classified as permanent prosthetics, augmentation devices or scaffolds [5]. It was observed that biological grafts undergo an initial phase of degradation and loss of strength followed by a phase in which they begin to get biologically incorporated. This motivated the development of ligament augmentation devices that are meant to provide initial mechanical support to the biological graft before it assimilates with the surrounding tissue [27]. On the other hand, while permanent prosthetic devices are meant to function as replacement without supporting tissue ingrowth; scaffolds are intended to provide both initial mechanical strength and support the eventual regeneration of load supporting soft tissue [10][22][28-29].

1.3.5 Tissue Engineered Ligament Grafts

Due to the above-mentioned drawbacks of biological and synthetic grafts, tissue engineered grafts have emerged as a potentially viable option for ACL replacement. The

optimal tissue engineered ligament graft would be a resorbable scaffold that promotes the regeneration of the damaged tissue eventually leading to the development of fully functional ligament that reproduces the long term mechanical and biological characteristics of the native ACL [10][30]. Both natural and synthetic polymers are being investigated for the development of viable tissue engineered grafts for ligament replacement.

A number of researchers have developed scaffolds of natural polymers, most commonly from collagen and silk [31][32]. The mechanical and degradation properties of natural scaffolds can be fairly easily altered based in the need by using various crosslinking methods. [5]. However, the mechanical properties of natural polymers are susceptible to deterioration when subjected to common sterilization procedures. Further, use of natural polymers is associated with higher risk of disease transmission and is typically more expensive compared to synthetic polymers [17][22]. Common synthetic resorbable polymers that have been used for the development for tissue engineering scaffolds include poly-L-lactic acid (PLLA) [33-34], poly(DTE carbonate) [35], polyglycolic acid PGA [34], polycaprolactone (PCL) [10], polyethylene glycol (PEG) based scaffolds [36], and polyurethane ureas (PUU) [35].

Laurencin et al. developed a three-dimensional braided scaffold composed of PLLA fibers. The braiding angle of these braided scaffolds was not uniform throughout the length of the scaffold. The scaffold had two bone attachment ends with a higher braiding angle and smaller pores compared to a central intra-articular region. This scheme was chosen to replicate the graded mechanical properties of the bone patellar tendon autograft [10]. Braided structures are generally used in applications where high axial stresses must

be born [37]. These scaffolds were able to transfer large loads, provide adequate extensions, and shear resistance [38]. Studies showed that these scaffolds retained 76% of their strength 4 weeks after implantation and 30% of their strength 6 weeks after implantation [33]. On the other hand, Ballock et al showed that patellar tendon autografts retained 6% and 15% of their strength after implantation for 6 weeks and 30 weeks, respectively [18].

Another relevant synthetic scaffold design developed by Freeman et al. involved the fabrication of a hierarchical braid-twist scaffold [39]. The twisting of fibers is approach generally adopted in the textile industry for yarns to withstand knitting processes. In general, increasing the twist of the yarn increases its abrasion resistance, however, beyond a certain maximal threshold the fibers become oriented along the short axis of the yarn resulting in a decrease in overall mechanical strength and abrasion properties [40].

1.4 Goal of the Project

The overall aim of the project was to develop and mechanically characterize a 3-D braided scaffold fabricated using a custom-braiding machine. In order to develop the scaffold the fiber twisting process previously developed by Freeman et al. was combined with a sequential 3-D braiding technique similar to Laurencin et al. After forming the 3-D braid twist scaffold the braiding angle of the scaffolds the braiding angles of the scaffolds will be altered. It was hypothesized that the hierarchical structure of the scaffold with an adjustable braiding angle would have mechanical properties that could be optimized to match those of the native human ACL.

CHAPTER 2 MATERIALS AND METHODS

2.1 Fabrication of 3-D Square Braid Twist Scaffolds

PLLA fibers purchased from Biomedical Structures were used to fabricate the 3-D square braid scaffolds. Each fiber was composed of 30 microfilaments. A 3-dimensional braid-twist scaffold was fabricated for this study. A schematic of the scaffold design is shown in [Figure 4**]**. Each scaffold is composed of 288 PLLA fibers. The fiber yarns were prepared using a method previously developed by Freeman et al [39]. Briefly, the purchased PLLA fibers were cut to lengths of 320 mm and were arranged into groups of four. Three groups of four fibers each were then twisted in a counterclockwise direction to form a fiber bundle with a twisting angle of 60±4.5°. These fiber bundles were subsequently twisted in a counterclockwise direction to form a yarn with a twisting angle of 72±2.3°. Earlier work by Freeman et al. showed that these twisting angles results in optimal mechanical properties for a fibrous PLLA-based ligament replacement [39]. The twisting of the fibers and fiber bundles was performed using a Conair twisting device (Model QB3ECS, Conair Corporation, East Windsor, NJ). Fibers were twisted for 5 seconds to form fiber bundles with the desired twisting angle, whereas fiber bundles were twisted for 3 seconds using device to form yarns having the desired twisting angle. Freeman et al. optimized these twisting times for fiber lengths of 16 cm [Figure 4]. However 32 cm fibers we used for this study, in order to obtain longer braids and improve the economy of the scaffold fabrication process. Therefore, the formation of the fiber bundles and yarns was carried out in two successive steps where 16 cm long sections of the 32 cm long fibers were twisted in each step. Twisting angles were

measured using a Leica inverted microscope. Twisting angles were defined as angle between the long axis of the fiber and the line perpendicular to the long axis of the yarn.

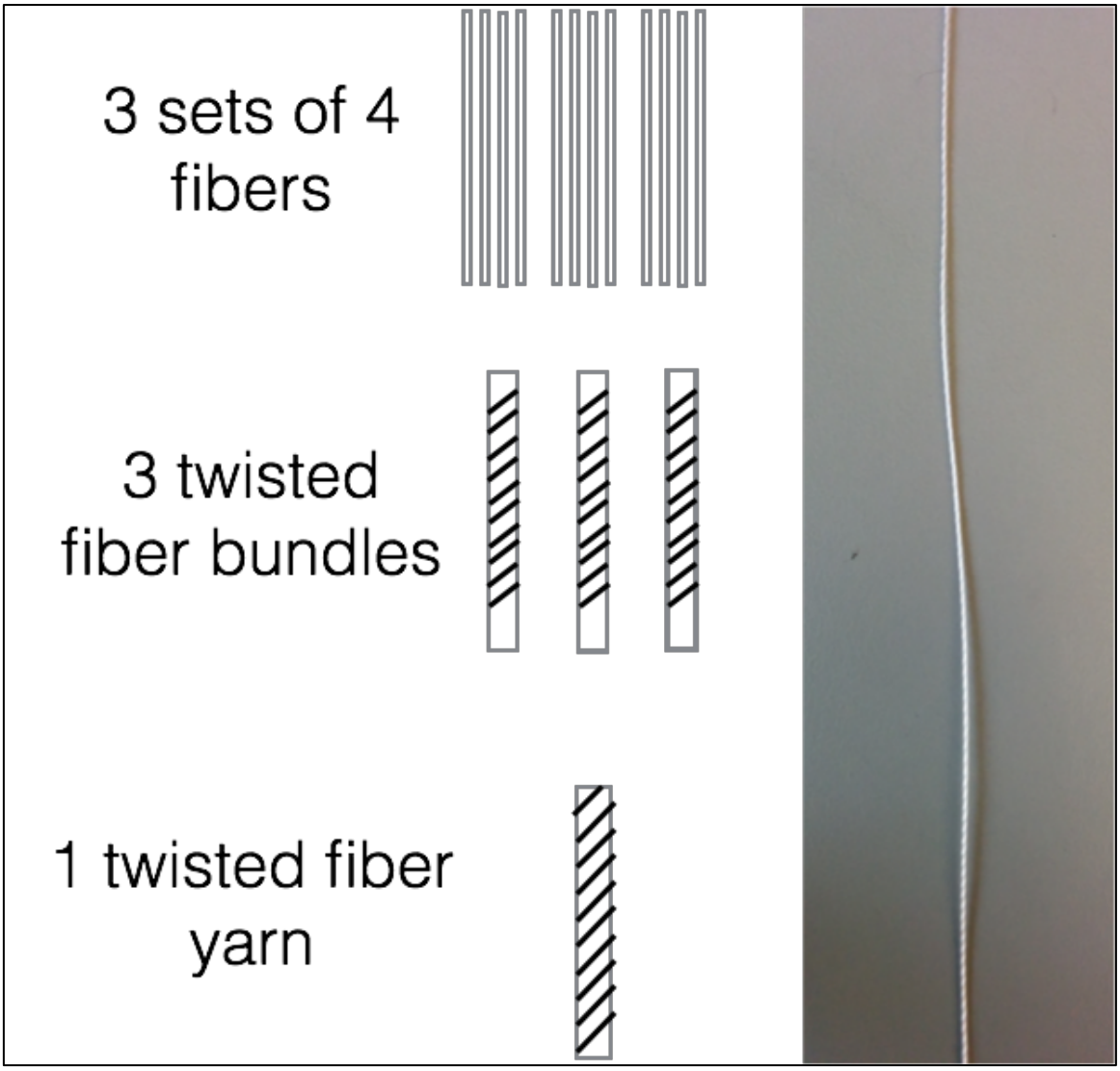

Figure 4: Left - Schematic representation of formation of PLLA yarns from fiber bundles and fibers. Right – Image of representative yarn

The fiber yarns were wound on the bobbins of the yarn carriers assembled on the braiding machine. The fiber bundles were then attached to a centrally located braiding point and were braided to form a square-shaped 3-D braid twist scaffold. The braiding point is defined as the point at which the yarns begin to get incorporated into the braid.

2.2 Description of Custom 3-D Braiding Machine and Square Braiding Process

The custom-braiding machine consists of yarn carriers placed on square-shaped loom. The yarn carriers move along rows and columns that are perpendicular to each other on a flat base also referred to as the machine bed. The carriers are assembled on movable tracks with slots in a specific alternating arrangement as shown in Figure 5. Braiding occurs by the cyclical movement of the yarn carriers on the machine bed. Pneumatic actuators consisting of a piston, an airtight cylinder and a gate valve, are used to move the carriers in a programmed pattern. The fiber yarns from all the yarn carriers are attached to a hook at the braiding point at the top of the machine. The formed braid is collected on a take-up spool placed directly above the braiding point.

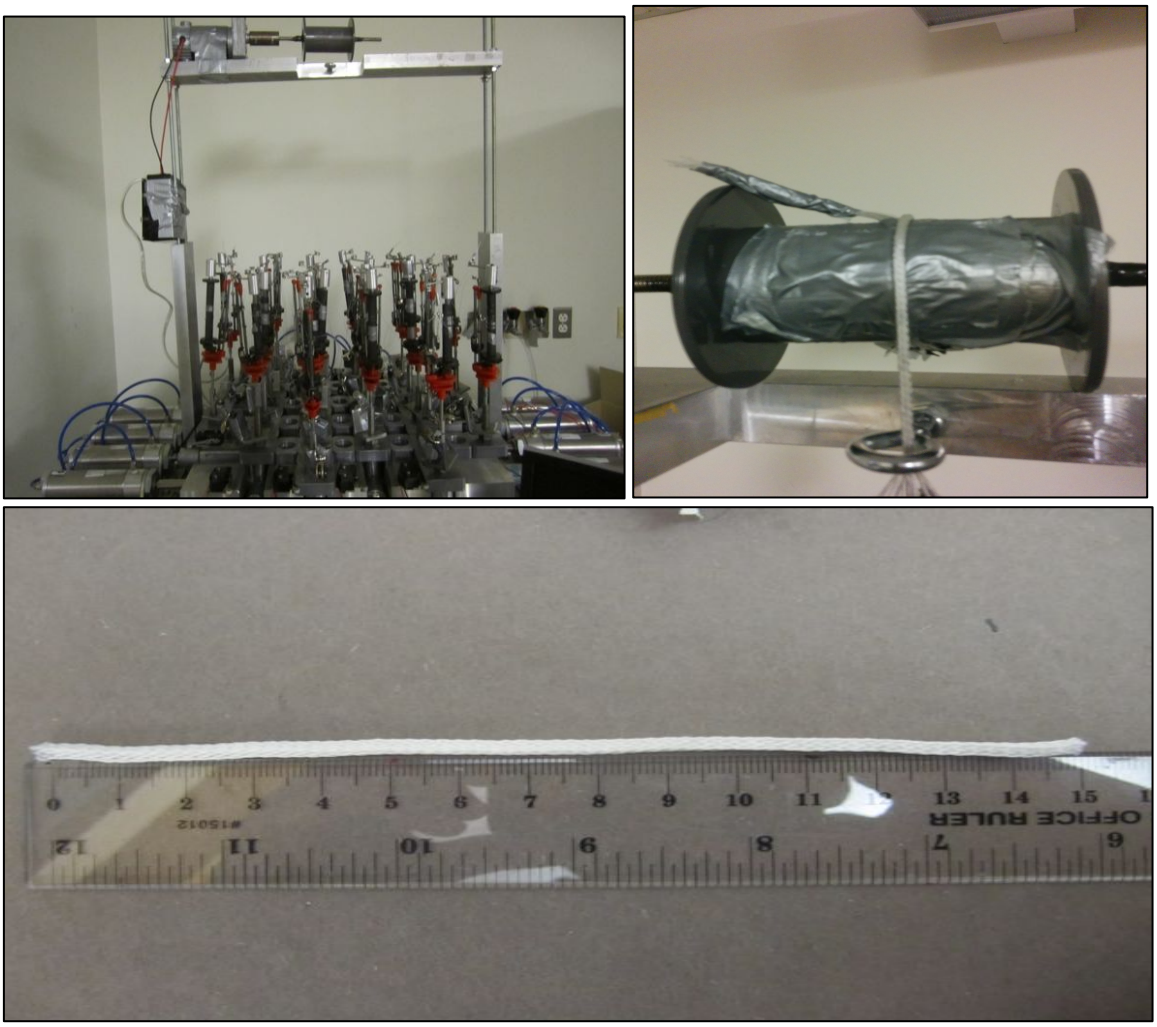

Figure 5: Top – Left - Image of braiding machine with alternating arrangement of yarn carrier. Top - Right – Braiding point with braid being collected on collecting spool. Bottom – Image of representative 72° scaffold

The specific pattern of movement of the yarn carriers on the machine bed determines the type of braid that is formed. A 3-D braiding technique called the 4-step process was used to form the 3-D square braids [37][41] [Figure 6]. The 4-step terminology refers to the four sequential carrier movement steps that make up one complete braiding cycle. In any one step of the process a particular yarn carrier will move only one step along either a row or a column. More specifically, step 1 results in motion of yarn carriers in alternating rows; step 2 involves motion of the carriers along alternating columns, while step 3 and step 4 results in a reverse of the motion of the rows in step 1 and columns in step 4

respectively. In all the above steps, yarn carriers in adjacent rows move in opposite directions relative to one another. After each step the yarns are subjected to a jamming action, which causes a tightly packed braid to be formed [42].

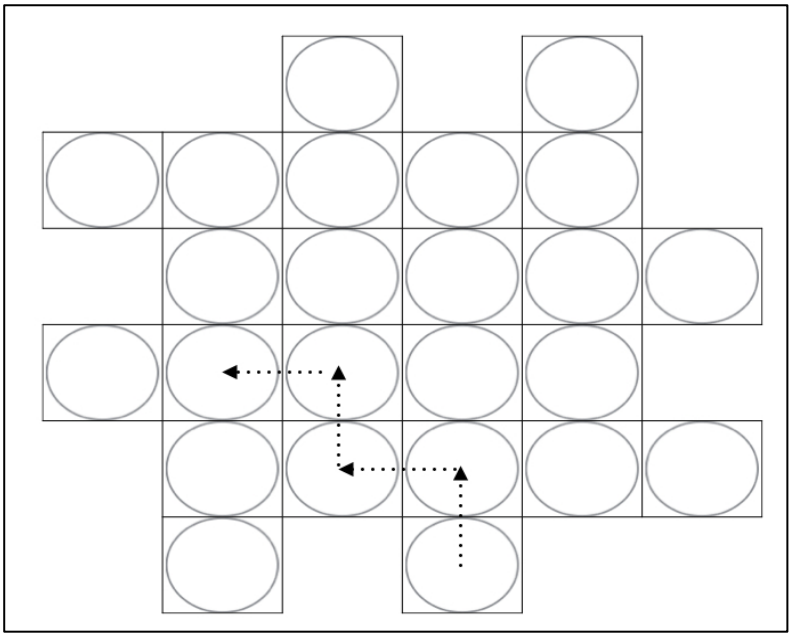

Figure 6: Schematic representation of movement of yarn carriers on the machine bed with the circles representing the carriers in the 4-step braiding process

2.3 Design of Custom-Modified Retractable Spools for Braiding Machine

Prefabricated carriers were purchased from Abhilash Enterprises Inc. Pune, India. The carriers consist of a vertical standard, a spindle and a freely rotating bobbin mounted on the spindles. The fiber bundles, prepared as mentioned above, are wound on the bobbin. The carrier is equipped with two guideposts fitted with coiled metal eyelets to guide the fiber bundle from the bobbin to the braiding point. Due to the cyclic motion of the carriers along the tracks and columns along the square base of the braiding machine, the distance between the braiding point and the top of the spindles that depends on the

location of the spindle relative to the braiding point. In general, this distance is smallest when a carrier is vertically underneath the braiding point, while it is largest when the carrier is located at the edges of the square frame of the braiding machine. This requires that the length of the fiber bundles be adjustable in response to the sequential movement of the yarn carrier. Moreover, it was observed that for adequate jamming or packing of the preform braid the fiber bundles need to be under constant tension during the entire braiding process in order for them to be properly incorporated into the 3-D braid.

However, the prefabricated carriers did not have sufficient retractability to keep the fiber bundles under constant tension for more than a few seconds into the braiding process. This would to a slackening of the fiber bundles during the operation of the braiding machine, resulting in either a complete failure of the braiding process or the formation of a highly irregular braided structure. In order to improve the retractability of the carriers while maintaining the fiber capacity of the carriers a modified design incorporating a weighted pulley was adopted as shown in Figure 7 below. This modification allowed the application of an adequate amount of tension to the fiber bundles without hampering the feeding of the bundles from the bobbin. The 3-D braids formed with these modified carriers had a regular structure and a uniform braiding angle throughout their length.

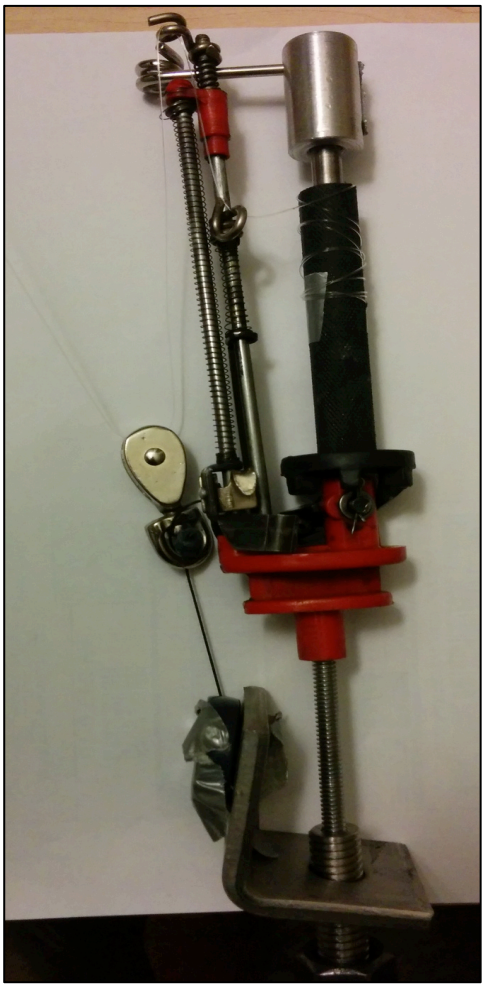

Figure 7: Modified design of yarn carrier with weighted pulley and guide post with eyelet

2.4 Variation of Braiding Angle

It was hypothesized that variations in the braiding angle could affect the influence the mechanical properties of the scaffold. The braiding point consisted of a hook attached to a steel bar spanning the width of the braiding machine above the yarn carriers. The steel bar was supported between a pair of long threaded steel rods on either end of the machine and was held in place by four adjustable positioning nuts. The height of the steel bar could be adjusted moving the positioning nuts along the threaded steel rods. It was hypothesized that varying the height of the steel bar and consequently, the height of the

braiding point that the braiding angle of the scaffold could be conveniently adjusted. Three different heights of the braiding point were used to determine their effect on the braiding angle of the scaffold. The braiding angle is defined as the angle made by the long axis of the yarns incorporated into middle of the braid and line perpendicular to the long axis of the scaffold as shown in Figure 8. Braiding angles were measured from at least six images taken along the length of the scaffold. Images were captured using a Nikon Coolpix Camera.

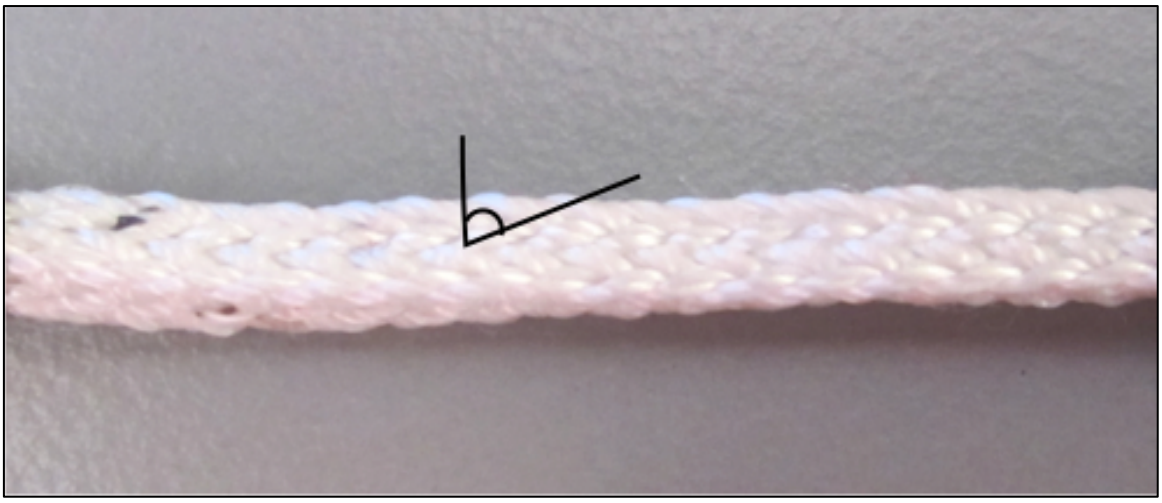

Figure 8: Representative image of 63° scaffold with braiding angle outlined

2.5 Tensile Testing of 3-D Square Braid Scaffolds

Uniaxial tensile tests were performed on the braided scaffolds using an INSTRON machine. The fabricated 3-D square braid scaffolds were cut to multiple samples each with a length of 4 cm. The ends of each sample were coated with a castable epoxy adhesive [Smooth On Inc., Easton PA]. This was done to prevent premature failure of the scaffold by ensuring that the grip anchors did not damage the scaffold during testing and by maintaining a constant cross sectional area throughout the length of the sample. Each sample was immersed in freshly prepared Phosphate Buffer Solution (PBS) for 1 hour

prior to testing. The scaffold samples were subsequently mounted on to the testing grips. The gauge length width and thickness dimensions of the sample were measure under a load 0.2 N. The sample was then pre-loaded to 3 N at a rate of 0.5 N/sec. Once the preload was reached the scaffold was extended to failure at a strain rate of 2 %/sec. Force displacement data was converted to stress-strain data in order to determine the ultimate tensile strength (UTS), the elastic modulus of the linear region of the stress-strain curve, the length of the toe-region and the strain at failure for each sample.

2.6 Statistical Analysis

Tensile testing data and braiding angle measurements were obtained for n=4 samples. One-way analysis of variance (ANOVA) and a pairwise Student's t-test were used to determine significant differences between test groups. A p-value < 0.05 was considered to be significant.

CHAPTER 3 Results

3.1 Scaffold Characteristics

This study has resulted in the design of a scaffold that combines techniques of fiber twisting and 3-D braiding to form a 3-D braid twist scaffold. Scaffolds with well-defined and uniform braiding angles were obtained. Adjusting the height of braiding point successfully altered the braiding angle of the 3-D braided scaffolds. It was observed that the braiding angle of the scaffolds increased with the height of the braiding point. The braiding angles of three different configurations of the scaffold are shown in Table 1. Scaffolds with mean braiding angles of 53°, 62° and 72° were obtained. The length of the scaffold obtained varied with braiding angles, with the 72°scaffold having the longest length (14 cm scaffold from 23 cm PLLA fiber yarns) while, the 53° scaffold was the shortest (12 cm from 23 cm PLLA fiber yarns). All scaffolds had approximately the same cross-sectional area.

Table 1: Braiding angle obtained for various heights of the braiding point.

Height of Braiding Point	Braiding Angle
16 cm	53.035±2.154
24 cm	63.01±2.654
31 cm	72.642±1.81

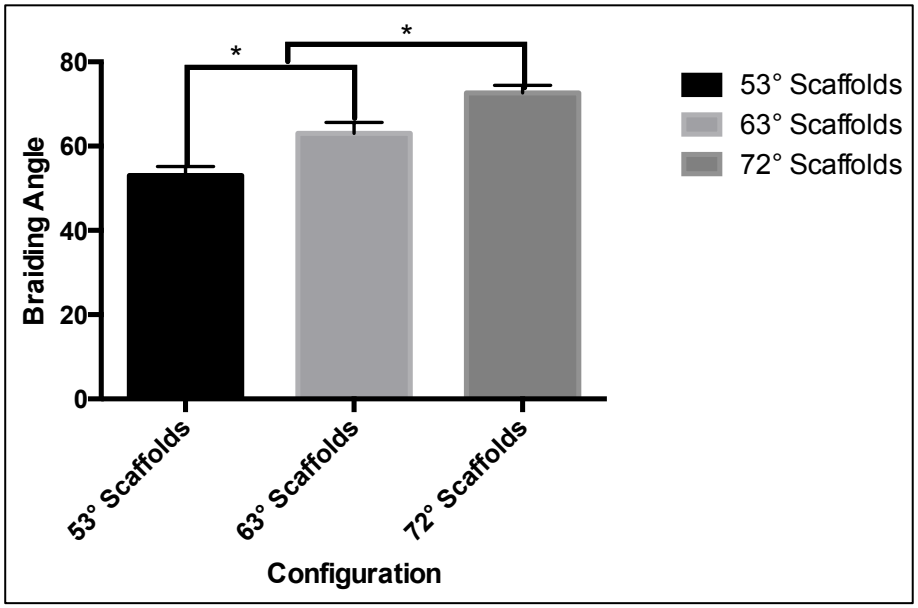

Figure 9: Comparison of braiding angles of the three configurations of the scaffolds

3.2 Tensile Properties of Scaffolds

The characteristic stress-strain curve from the tensile testing of the scaffolds is shown in Figure 10: Characteristic stress-strain curve of the 3-D braid twist scaffold. It was observed that all scaffolds had a toe region, followed by a linear region and a yield region before failure. Data from the stress strain curves is used to determine the ultimate tensile strength (UTS), the elastic modulus of the linear region of the stress-strain curve, the length of the toe-region and the strain at failure for each sample.

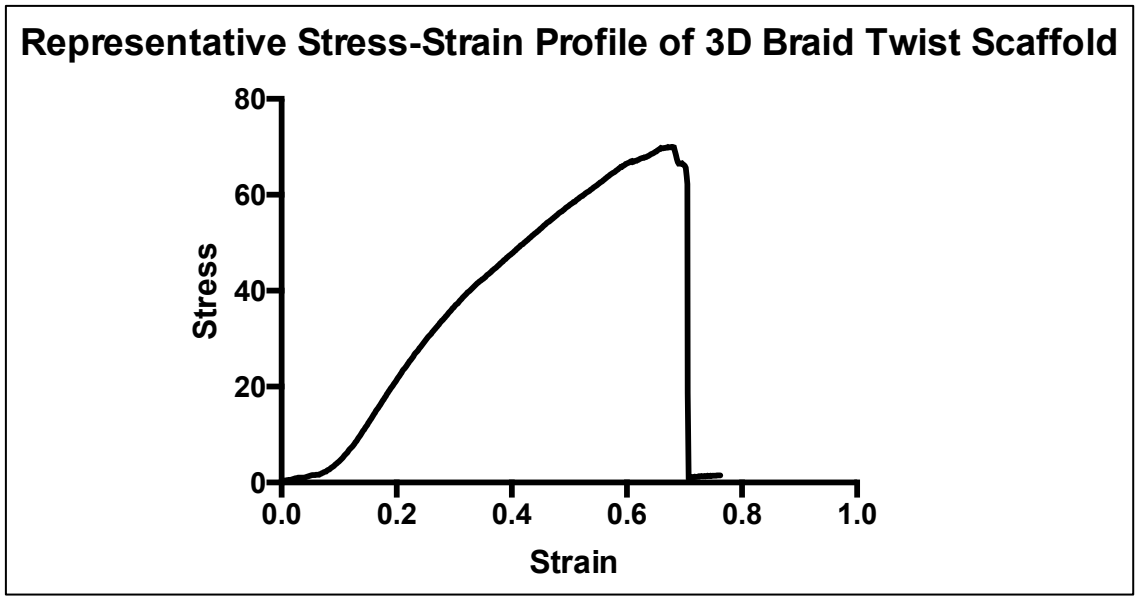

Figure 10: Characteristic stress-strain curve of the 3-D braid twist scaffold

Results from the tensile tests revealed that ultimate tensile strength (UTS) of the scaffolds varied from about 63.6 MPa to about 79.5 MPa. However, there were no significant differences in UTS between scaffolds having different braiding angles [Figure 11**]**. Furthermore, there was no significant change in the length of the toe region of the scaffolds with braiding angle although there was a trend of decreasing length of toe region with increasing braiding angle [Figure 11**]**. The toe regions of the scaffolds varied from about 5% to about 9% strain (5.9±0.75% for the 72° scaffold, 6.81±1.7% for the 62° scaffold, and 7.15±1.66% for the 53° scaffold).

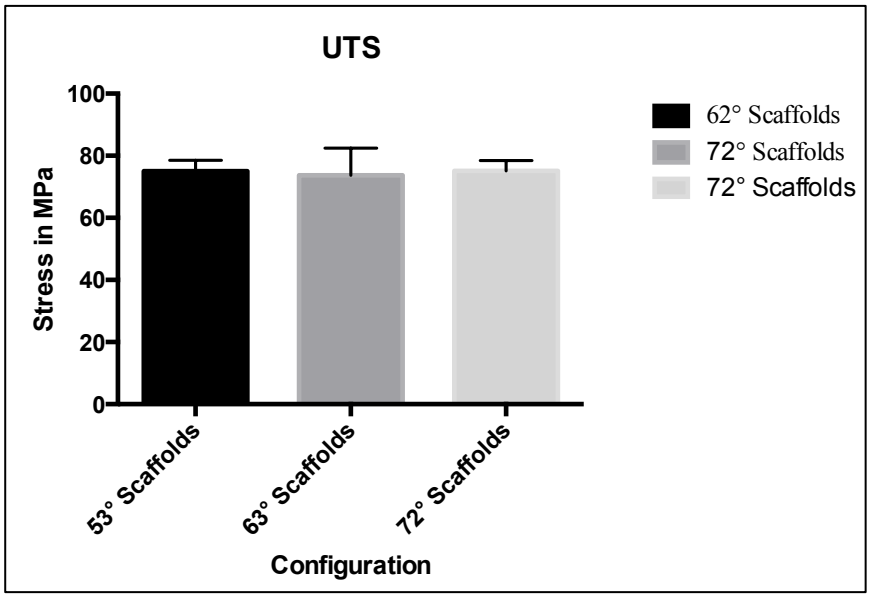

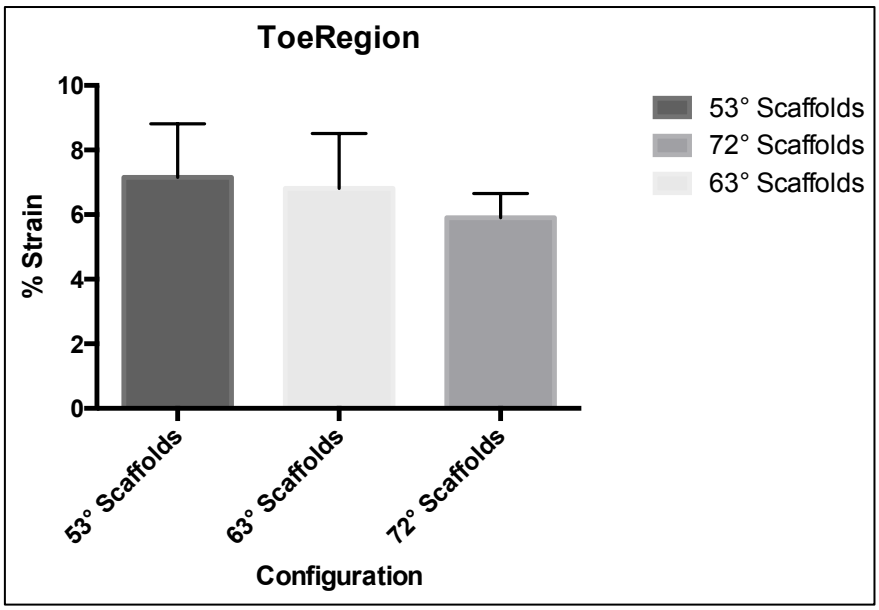

Figure 11: Top - UTS of scaffolds. Bottom – Length of the toe region of the scaffolds

The modulus of the linear region of the stress-strain curve decreased with the braiding angle. The Young's modulus of the linear region for the 53° scaffold (246.1056± 45.6173 MPa) was significantly lower than that for the 72° scaffold (363.7702±56.0025 MPa) [Figure 12]. On the other hand there was an increase in the strain at failure with decreasing braiding angle of the scaffolds [Figure 13].

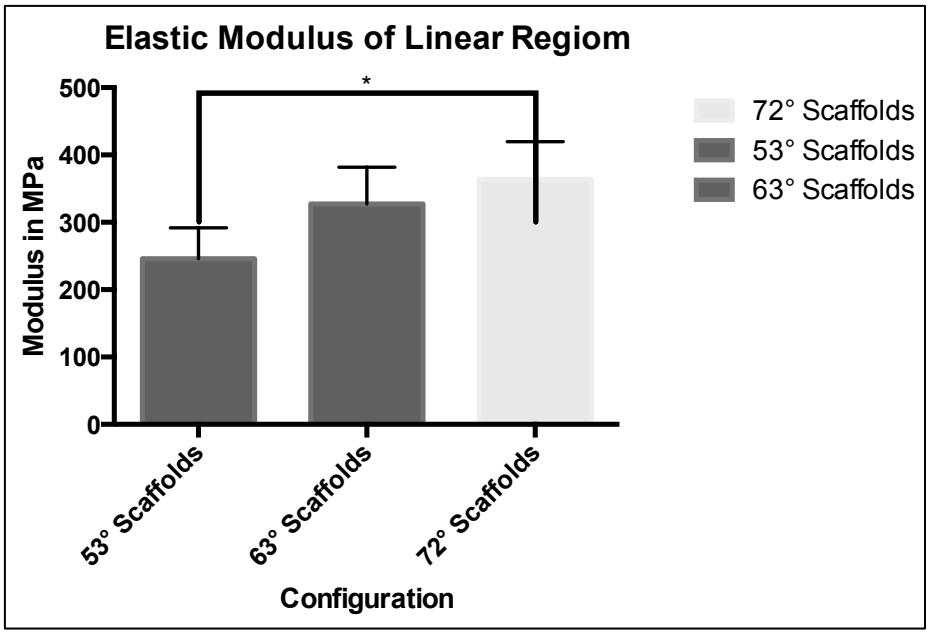

Figure 12: Elastic modulus of the linear region of the scaffolds

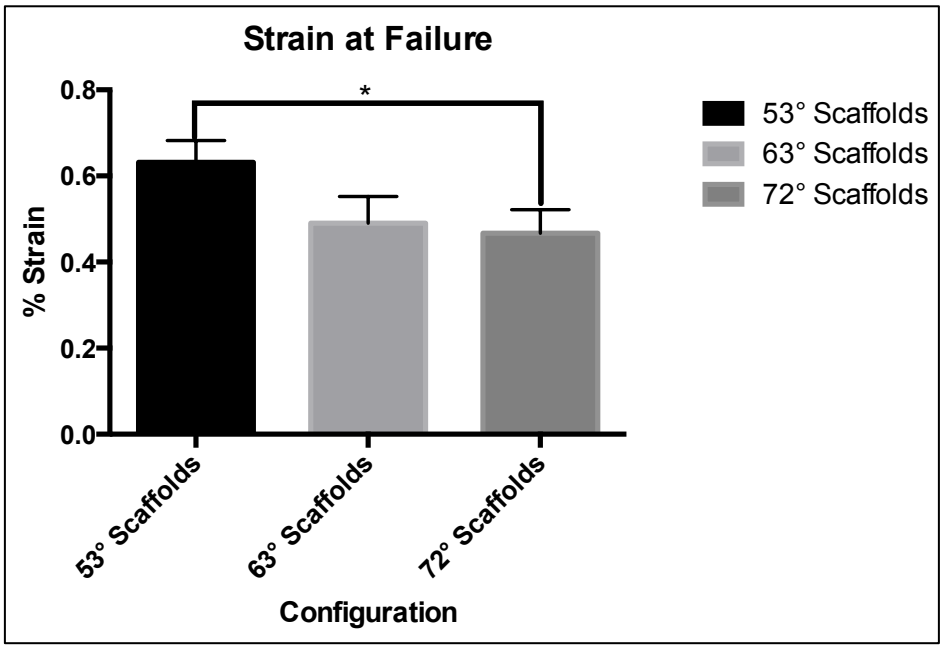

Figure 13: Strain at failure for scaffolds with various braiding angles

CHAPTER 4 DISCUSSION

It is necessary for synthetic ligament grafts to recapitulate the mechanical and biological properties of the native ACL to achieve successfully functional replacement. A range of values exist for he UTS and the elastic modulus of the linear region of native ACLs. Noyes et al. have reported the ultimate tensile strength of ACLs from younger donors to be 37.8±9.3 MPa [43]. In a study by Butler et al. the UTS of the posterolateral and anteromedial bundles of the human ACL were compared [44]. The anterior unit was found to have an average UTS of 38 MPa, while the posterior unit had an average UTS of 15 MPa. In order to withstand the physiological stresses experienced by the native ligament while experiencing degradation, the ultimate tensile strength of the scaffolds should be equal to or greater than that of the native ACL. The UTS of all three configurations of the 3-D braid twist scaffolds evaluated in this study (ranging from 63.6 MPa -79.5 MPa) exceeded that of the native ACL.

Previous studies have shown that human ACLs and medial collateral ligaments (MCL) display two regions from 2% to 4.8% strain [45-47]. Our 3-D braid twist scaffolds exhibited a range of toe regions from about 5% strain to about 9% strain. Although there were no significant differences between the groups there was a general trend of a decrease in the length of the toe region of the scaffolds with increase in the braiding angle. The 72° scaffolds had a toe region of 5.9±0.75% strain and is most similar to the reported values of the native human ligaments [Table 2].

Noyes et al. reported that modulus of the linear region of ACLs to be 111 ± 26 MPa, while Butler et al. found the anterior and posterior bundles of the ligament to have

average moduli of 284 MPa and 154 MPa, respectively, with an average of 278 MPa. The tensile modulus of all configurations of the scaffolds was very similar to these reported values. The elastic modulus of the scaffolds increased with an increase in the braiding angle. The 53° scaffolds had an elastic modulus that was closest to the values reported in literature. However, it is known that scaffold mechanical properties tend to decrease after implantation [10][33]. Furthermore, future generations of these scaffolds might include a hydrogel component in order to enhance their viscoelastic response. Previous studies by Freeman et al. have shown that the addition of a poly(ethylene glycol) diacrylate (PEGDA) hydrogel to fibrous planar braided PLLA scaffolds led to a decrease in their UTS [36]. Thus, in order to increase their long-term mechanical function scaffolds should be optimized for maximal tensile modulus. Therefore, based on all of the above mentioned mechanical design criteria the 72° scaffold with a modulus of 363.7702±56.0025 MPa, a toe region of 5.9±0.75% strain, an ultimate strain of 46.67±5.51 %strain and UTS of 75.1226±3.3039 MPa was found to be the most promising configuration for ACL replacement.

Table 2: Comparison of Tensile properties of native human ACL with those of the 72° 3-D braid twist scaffolds

Property	**72° Scaffolds**	**Native ACL [43]**
UTS	75.123±3.304 MPa	37.8±9.3 MPa
Toe Region	5.9±0.75% Strain	2-4.8% Strain
Elastic Modulus	363.77±55.06 MPa	111±26 MPa
Strain at Failure	46.7±5.51% Strain	~44.3±8.5% Strain

CHAPTER 5 CONCLUSION AND FUTURE WORK

3-D square braid twist scaffolds were successfully fabricated by combining previously developed fiber twisting technique by Freeman et al. [39] and a 3-D braiding technique adapted from Laurencin et al [38]. This scaffold was able to mimic the biomechanical behavior of the native ACL. However, a complete mechanical and biological characterization of the scaffolds is necessary to determine their suitability for ACL replacement. Further investigations into the stress relaxation behavior of the scaffolds would be required. It is expected that the addition of a biocompatible hydrogel component, like PEGDA, could serve to optimize the viscoelastic behavior of the scaffold. Further in vitro and in vivo biological characterization is required to determine the ultimate suitability of the scaffold to promote tissue ingrowth and replicate the mechanical properties of the native human ACL in the long-term.

REFERENCES

[1] Y. M. Ml Cameron, "Diagnosing and managing anterior cruciate ligament injuries."

[2] S. M. Gianotti, S. W. Marshall, P. A. Hume, and L. Bunt, "Incidence of anterior cruciate ligament injury and other knee ligament injuries: a national population-based study," *J. Sci. Med. Sport Sports Med. Aust.*, vol. 12, no. 6, pp. 622–627, Nov. 2009.

[3] W. Petersen and T. Zantop, "Anatomy of the anterior cruciate ligament with regard to its two bundles," *Clin. Orthop.*, vol. 454, pp. 35–47, Jan. 2007.

[4] M. Takahashi, M. Doi, M. Abe, D. Suzuki, and A. Nagano, "Anatomical study of the femoral and tibial insertions of the anteromedial and posterolateral bundles of human anterior cruciate ligament," *Am. J. Sports Med.*, vol. 34, no. 5, pp. 787–792, May 2006.

[5] V. I. Walters, "Design and Analysis of a Collagenous Anterior Cruciate Ligament Replacement," 26-May-2011. [Online]. Available: http://scholar.lib.vt.edu/theses/available/etd-05092011-124821/. [Accessed: 12-Dec-2014].

[6] F. H. Fu, C. D. Harner, D. L. Johnson, M. D. Miller, and S. L. Woo, "Biomechanics of knee ligaments: basic concepts and clinical application," *Instr. Course Lect.*, vol. 43, pp. 137–148, 1994.

[7] B. A. Smith, G. A. Livesay, and S. L. Woo, "Biology and biomechanics of the anterior cruciate ligament," *Clin. Sports Med.*, vol. 12, no. 4, pp. 637–670, Oct. 1993.

[8] C. D. Harner, G. H. Baek, T. M. Vogrin, G. J. Carlin, S. Kashiwaguchi, and S. L.-Y. Woo, "Quantitative Analysis of Human Cruciate Ligament Insertions," *Arthrosc. J. Arthrosc. Relat. Surg.*, vol. 15, no. 7, pp. 741–749, Oct. 1999.

[9] C. B. Frank, "Ligament structure, physiology and function," *J. Musculoskelet. Neuronal Interact.*, vol. 4, no. 2, pp. 199–201, Jun. 2004.

[10] C. T. Laurencin and J. W. Freeman, "Ligament tissue engineering: An evolutionary materials science approach," *Biomaterials*, vol. 26, no. 36, pp. 7530–7536, Dec. 2005.

[11] *Biomaterials, Medical Devices and Tissue Engineering: An Integrated Approach - An integrated approach*. .

[12] H. E. Cabaud, W. G. Rodkey, and J. A. Feagin, "Experimental studies of acute anterior cruciate ligament injury and repair," *Am. J. Sports Med.*, vol. 7, no. 1, pp. 18–22, Feb. 1979.

[13] Y. Liu, H. S. Ramanath, and D.-A. Wang, "Tendon tissue engineering using scaffold enhancing strategies," *Trends Biotechnol.*, vol. 26, no. 4, pp. 201–209, Apr. 2008.

[14] J. Diamant, A. Keller, E. Baer, M. Litt, and R. G. C. Arridge, "Collagen; Ultrastructure and Its Relation to Mechanical Properties as a Function of Ageing," *Proc. R. Soc. Lond. B Biol. Sci.*, vol. 180, no. 1060, pp. 293–315, Mar. 1972.

[15] D. J. McBride Jr, R. A. Hahn, and F. H. Silver, “Morphological characterization of tendon development during chick embryogenesis: measurement of birefringence retardation,” *Int. J. Biol. Macromol.*, vol. 7, no. 2, pp. 71–76, Apr. 1985.
[16] E. Mosler, W. Folkhard, E. Knörzer, H. Nemetschek-Gansler, T. Nemetschek, and M. H. Koch, “Stress-induced molecular rearrangement in tendon collagen,” *J. Mol. Biol.*, vol. 182, no. 4, pp. 589–596, Apr. 1985.
[17] A. L. Kwansa, Y. M. Empson, E. C. Ekwueme, V. I. Walters, J. W. Freeman, and C. T. Laurencin, “Novel matrix based anterior cruciate ligament (ACL) regeneration,” *Soft Matter*, vol. 6, no. 20, p. 5016, 2010.
[18] R. T. Ballock, S. L. Woo, R. M. Lyon, J. M. Hollis, and W. H. Akeson, “Use of patellar tendon autograft for anterior cruciate ligament reconstruction in the rabbit: a long-term histologic and biomechanical study,” *J. Orthop. Res. Off. Publ. Orthop. Res. Soc.*, vol. 7, no. 4, pp. 474–485, 1989.
[19] H. Segawa, G. Omori, and Y. Koga, “Long-term results of non-operative treatment of anterior cruciate ligament injury,” *The Knee*, vol. 8, no. 1, pp. 5–11, Mar. 2001.
[20] J. O. Hollinger, *An Introduction to Biomaterials, Second Edition*. CRC Press, 2011.
[21] D. M. Daniel, W. H. Akeson, and J. J. O’Connor, Eds., *Knee ligaments: structure, function, injury, and repair*. New York: Raven Press, 1990.
[22] J. W. Freeman, “Tissue Engineering Options for Ligament Healing,” *Bone Tissue Regen. Insights*, vol. 2009, no. 2, pp. 13–23, Sep. 2009.
[23] D. W. Jackson, J. T. Heinrich, and T. M. Simon, “Biologic and synthetic implants to replace the anterior cruciate ligament,” *Arthroscopy*, vol. 10, no. 4, pp. 442–452, Aug. 1994.
[24] B. D. Beynnon, R. J. Johnson, J. A. Abate, B. C. Fleming, and C. E. Nichols, “Treatment of anterior cruciate ligament injuries, part I,” *Am. J. Sports Med.*, vol. 33, no. 10, pp. 1579–1602, Oct. 2005.
[25] F. R. Noyes, D. L. Butler, E. S. Grood, R. F. Zernicke, and M. S. Hefzy, “Biomechanical analysis of human ligament grafts used in knee-ligament repairs and reconstructions,” *J. Bone Joint Surg. Am.*, vol. 66, no. 3, pp. 344–352, Mar. 1984.
[26] K. R. Stone, U. M. Abdel-Motal, A. W. Walgenbach, T. J. Turek, and U. Galili, “Replacement of human anterior cruciate ligaments with pig ligaments: a model for anti-non-gal antibody response in long-term xenotransplantation,” *Transplantation*, vol. 83, no. 2, pp. 211–219, Jan. 2007.
[27] K. Kumar and N. Maffulli, “The ligament augmentation device: an historical perspective,” *Arthrosc. J. Arthrosc. Relat. Surg. Off. Publ. Arthrosc. Assoc. N. Am. Int. Arthrosc. Assoc.*, vol. 15, no. 4, pp. 422–432, May 1999.
[28] R. Mascarenhas and P. B. MacDonald, “Anterior cruciate ligament reconstruction: a look at prosthetics - past, present and possible future,” *McGill J. Med. MJM*, vol. 11, no. 1, pp. 29–37, Jan. 2008.
[29] L. Ambrosio, R. De Santis, and L. Nicolais, “Composite hydrogels for implants,” *Proc. Inst. Mech. Eng. [H]*, vol. 212, no. 2, pp. 93–99, 1998.
[30] F. Van Eijk, D. B. F. Saris, J. Riesle, W. J. Willems, C. A. Van Blitterswijk, A. J. Verbout, and W. J. A. Dhert, “Tissue engineering of ligaments: a comparison of

bone marrow stromal cells, anterior cruciate ligament, and skin fibroblasts as cell source," *Tissue Eng.*, vol. 10, no. 5–6, pp. 893–903, Jun. 2004.
[31] V. I. Walters, A. L. Kwansa, and J. W. Freeman, "Design and Analysis of Braid-Twist Collagen Scaffolds," *Connect. Tissue Res.*, vol. 53, no. 3, pp. 255–266, Jun. 2012.
[32] B. B. Mandal, S.-H. Park, E. S. Gil, and D. L. Kaplan, "Multilayered silk scaffolds for meniscus tissue engineering," *Biomaterials*, vol. 32, no. 2, pp. 639–651, Jan. 2011.
[33] J. A. Cooper, J. S. Sahota, W. J. Gorum, J. Carter, S. B. Doty, and C. T. Laurencin, "Biomimetic tissue-engineered anterior cruciate ligament replacement," *Proc. Natl. Acad. Sci.*, vol. 104, no. 9, pp. 3049–3054, Feb. 2007.
[34] H. H. Lu, J. A. Cooper Jr., S. Manuel, J. W. Freeman, M. A. Attawia, F. K. Ko, and C. T. Laurencin, "Anterior cruciate ligament regeneration using braided biodegradable scaffolds: in vitro optimization studies," *Biomaterials*, vol. 26, no. 23, pp. 4805–4816, Aug. 2005.
[35] S. L. Bourke, J. Kohn, and M. G. Dunn, "Preliminary development of a novel resorbable synthetic polymer fiber scaffold for anterior cruciate ligament reconstruction," *Tissue Eng.*, vol. 10, no. 1–2, pp. 43–52, Feb. 2004.
[36] J. W. Freeman, M. D. Woods, D. A. Cromer, E. C. Ekwueme, T. Andric, E. A. Atiemo, C. H. Bijoux, and C. T. Laurencin, "Evaluation of a hydrogel–fiber composite for ACL tissue engineering," *J. Biomech.*, vol. 44, no. 4, pp. 694–699, Feb. 2011.
[37] T.-W. Chou and F. K. Ko, Eds., *Textile structural composites*. Amsterdam ; New York : New York, NY, U.S.A: Elsevier ; Distributors for the U.S. and Canada, Elsevier Science Pub. Co, 1989.
[38] J. A. Cooper, "Design, optimization and in vivo evaluation of a tissue-engineered anterior cruciate ligament replacement."
[39] J. W. Freeman, M. D. Woods, and C. T. Laurencin, "Tissue Engineering of the Anterior Cruciate Ligament Using a Braid-Twist Scaffold Design," *J. Biomech.*, vol. 40, no. 9, pp. 2029–2036, 2007.
[40] M. L. Joseph, *Joseph's introductory textile science*, 6th ed. Fort Worth: Harcourt Brace Jovanovich College Publishers, 1992.
[41] F. K. Ko, C. M. Pastore, and A. A. Head, *Atkins and Pearce Handbook of Industrial Braiding*. Atkins & Pearce, 1989.
[42] X. ZHENG and T. YE, "Microstructure Analysis of 4-Step Three-Dimensional Braided Composite," *Chin. J. Aeronaut.*, vol. 16, no. 3, pp. 142–150, Aug. 2003.
[43] F. R. Noyes and E. S. Grood, "The strength of the anterior cruciate ligament in humans and Rhesus monkeys," *J. Bone Joint Surg. Am.*, vol. 58, no. 8, pp. 1074–1082, Dec. 1976.
[44] D. L. Butler, Y. Guan, M. D. Kay, J. F. Cummings, S. M. Feder, and M. S. Levy, "Location-dependent variations in the material properties of the anterior cruciate ligament," *J. Biomech.*, vol. 25, no. 5, pp. 511–518, May 1992.
[45] M. Dienst, R. T. Burks, and P. E. Greis, "Anatomy and biomechanics of the anterior cruciate ligament," *Orthop. Clin. North Am.*, vol. 33, no. 4, pp. 605–620, v, Oct. 2002.

[46] C. Bonifasi-Lista, S. P. Lake, M. S. Small, and J. A. Weiss, “Viscoelastic properties of the human medial collateral ligament under longitudinal, transverse and shear loading,” *J. Orthop. Res. Off. Publ. Orthop. Res. Soc.*, vol. 23, no. 1, pp. 67–76, Jan. 2005.
[47] L. Ambrosio, R. De Santis, S. Iannace, P. A. Netti, and L. Nicolais, “Viscoelastic behavior of composite ligament prostheses,” *J. Biomed. Mater. Res.*, vol. 42, no. 1, pp. 6–12, Oct. 1998.